Environmental Science and Pollution Research (2020) 27:12332–12344
https://doi.org/10.1007/s11356-020-07800-w

RESEARCH ARTICLE

Improving the performance of solar still using different heat localization materials

Swellam Wafa Sharshir[1] · Ammar Hamed Elsheikh[2] · Youssef Mustafa Ellakany[1] · Abdallah Wagih Kandeal[1] · Elbager Mohammed Awadalla Edreis[3,4] · Ravishankar Sathyamurthy[5] · Amrit Kumar Thakur[6] · Mohamed Abdelaziz Eltawil[7,8] · Mofreh Hamada Hamed[1,9] · Abd Elnaby Kabeel[10]

Received: 29 October 2019 / Accepted: 21 January 2020 / Published online: 28 January 2020

Abstract

This work aimed to explore a new technique for improving the performance of solar stills (SSs) through utilizing three different types of a new hybrid structure of heat localization materials (HSHLM) floating on the water surface to increase the evaporation rate as well as water production and minimize heat losses. The three types were exfoliated graphite flakes with wick (type A), carbon foam with wick (type B), and exfoliated graphite flakes with wick and carbon foam (type C). These hybrid structures had good features such as high absorption and hydrophilic capillary forces to interconnected pores for fluid flow through the structure. Two identical SSs were designed, fabricated, and investigated to assess SSs' performance with and without HSHLM (modified and conventional SSs). The obtained results showed that the daily productivity was enhanced by 34.5, 28.6, and 51.8% for type A, type B, and type C, respectively, relative to the conventional one. Moreover, the efficiency of the SS reached about 37.6% for type C; while, it reached about 27% for the conventional SS. Contrary to conventional SSs, the use of HSHLM resulted in increasing the productivity proportional to water depth.

Keywords Solar desalination · Heat localization materials · Exfoliated graphite · Carbon foam · Wick

Introduction

Fresh water is essential for urban expansion, human civilization, and industrial development (Nisan and Benzarti 2008). Water covers around 70% of the globe while most of this water is not suitable for drinking because of salinity and water pollution (El-Samadony and Kabeel 2014). So, the fresh water demand is increasing, and the existing sources cannot be enough to meet these increasing demands (Kabeel et al., 2017a). Good water quality is needed to enhance the level of living. Water gets mainly contaminated due to the industrial activities causing severe diseases, which can affect our life. To solve this immense problem, many advanced technologies have been employed, but they are very expensive (Rodriguez-Narvaez et al. 2017; Salgot and Folch

Responsible editor: Philippe Garrigues

✉ Abd Elnaby Kabeel
kabeel6@hotmail.com; kabeel6@f-eng.tanta.edu.eg

Swellam Wafa Sharshir
sharshir@eng.kfs.edu.eg

[1] Mechanical Engineering Department, Faculty of Engineering, Kafrelsheikh University, Kafrelsheikh 33516, Egypt

[2] Production Engineering and Mechanical Design Department, Faculty of Engineering, Tanta University, Tanta, Egypt

[3] Mechanical Engineering Department, Faculty of Engineering, University of Blue Nile, Blue Nile Roseires, Al-Roseires, Sudan

[4] Department of Mechanical Engineering, Alsalama College of Sciences & Technology (ACST), Khartoum Bahri, Sudan

[5] Department of Automobile Engineering, Hindustan Institute of Technology and Science, Chennai, Tamil Nadu 603103, India

[6] Mechanical Engineering Department, CEG Campus, Anna University, Chennai, Tamil Nadu 600025, India

[7] Agricultural Engineering Department, Faculty of Agriculture, Kafrelsheikh University, Kafrelsheikh 33516, Egypt

[8] Department of Agricultural Systems Engineering, College of Agricultural and Food Sciences, King Faisal University, P.O.Box 420Al-Hofuf Al-Ahsa 31982, Saudi Arabia

[9] Higher Institute of Engineering and Technology, MNF-HIET, Menoufia, Egypt

[10] Mechanical power Engineering Department, Faculty of Engineering, Tanta University, Tanta, Egypt

2018; T. C et al. 2018). Therefore, solar energy as a promising abundant source of renewable energy has attracted the attention of many researchers in the water desalination field (Abujazar et al. 2018; Elsheikh et al. 2018; Li et al. 2013; Zhang et al. 2018).

Solar stills (SSs) are one of the most promising solutions to water purification especially in remote areas when a small amount is needed (Ayoub and Malaeb 2014; Samuel Hansen and Kalidasa Murugavel 2017; Sharshir et al. 2017a). The major disadvantage of SSs is the low rate of productivity, in spite of continued efforts done by many different researches to improve their performance through different designs and modifications (Balachandran et al. n.d. ; Elshamy and El-Said 2018; Shalaby et al. 2016; Sharshir et al. 2016d). The parameters that significantly affect SSs performance and efficiency are location, wind velocity, solar intensity, water depth, glass temperature, and ambient temperature (Kabeel et al. 2019c). The main disadvantage of SSs is that productivity is low. This low productivity is mainly due to two reasons: the latent heat losses of water condensation and the low insolation received by SS. Further developments of the SSs have been done to enhance their performance such as using phase change materials (PCM) to store energy during the daytime and release it during the night (Kabeel et al. 2018; Kabeel et al. 2017b; Mousa and Gujarathi 2016; Su et al. 2015). Recently the researchers have extensively used micro-nano particles to improve the SS performance (Balachandran et al. 2019; Elsheikh et al. 2019; Kabeel et al. 2019b; Rashidi et al. 2018; Sharshir et al. 2017c). Sharshir et al. (2017b) proposed the use of graphite flakes and phase change material in the still basin integrated with film cooling over the glass cover which improved water productivity by about 73.80%. To enhance the water evaporation as well as productivity, researchers have been investigated the using of phase change material integrated with nanoparticles to exploit the advantages of both of them(Dsilva Winfred Rufuss et al. 2018), and the use of porous absorber (Arunkumar et al. 2018; Madani and Zaki 1995) to increase the evaporative surface area of the basin. In addition, different heat storage materials have been considered for improving the productivity such as cement-coated red bricks (Kabeel et al. 2019a), solar evaporation using airing multifunctional textile (Peng et al. 2020), v-corrugated absorber integrated with wick and nanofluids (Sharshir et al. 2020), cotton hung pad integrated with nanoparticles (Sharshir et al. 2019a), heat-localization and thin-film evaporation (Peng et al. 2018) metal chips pad and basin metals (Sharshir et al. 2019d), improving solar still performance via water rejected from humidification-dehumidification (Sharshir et al. 2016a, b, c), phase change materials (Sharshir et al. 2019b).

Khare et al. (2017) investigated the effect of using black rubber and black gravel inside the still trough on SS productivity which was enhanced by 20% and 19% for the former and the latter, respectively. Hassan and Abo-Elfadl (2017) reported an increase in SS productivity up to 35% when saturated sand, layers of black steel fiber, and a mixture of both in the basin medium were used. Moreover, mixing the sand with black steel fibers showed higher productivity compared with sand only. Samuel Hansen and Kalidasa Murugavel (2017) tested different types of absorber plates (flat, grooved, and fined shaped). The distillate water productivity and efficiency using fined shaped absorber were higher than the standard flat absorber by 25.7% and 34.1%, respectively.

Heat localization as a new technique has been used to increase water evaporation in open space showed great promises in the desalination field. By localizing the solar energy on the water surface using a different kinds of materials, the surface of water gets heated effectively leading to generate vapor. Wang et al. (2016) reported an increase in the evaporation rate of water by localizing heat on the water surface using carbon nanotubes. The evaporation efficiency in open air was 46.8% under 10 kW/m^2 of insolation. Later, Xue et al. (2017) used flame treated wood as a low-cost material for localizing heat in a steam generating device which showed thermal efficiency of 72% at under 1 kW/m^2 of insolation in open space.

Considering low-cost materials, Xu et al. (2017) used natural and carbonized mushrooms as heat localization materials to generate steam which showed efficiencies of 62% and 78% under 1 kW/m^2 of insolation, respectively. (Ghasemi et al. 2014) proposed a hydrophilic exfoliated structure for increasing water evaporation 10 kW/m^2 of insolation using a solar simulator on an open environment. The results indicated that the maximum efficiency was about 85%. Liu et al. (2017) reported that 1.2 kg of salty water can be vaporized in 1 h using dark met surface composed of nanoparticles with a thickness of 200 mm, and the thermal efficiency was 87% under 2.3 kW/m^2 of insolation.

It has been observed from the literature that heat localization techniques will be beneficial to the performance of SSs. The present experimental works aim to develop a new approach and corresponding material structure that localizes the heat at the surface, where evaporation occurs, and minimize the heat losses leading to enhance the thermal performance of the SSs. Three different types of HSHLMs, namely, exfoliated graphite flakes with wick (type A), carbon foam with wick (type B), and exfoliated graphite flakes with wick and carbon foam (type C), were used to achieve the heat localization. Using these types of HSHLM forms hot spots by concentrating the solar radiation on the water surface, hence it reduces the heat loss leading to enhance thermal efficiency. Furthermore, the effect of water depth on the productivity of modified and conventional SSs was investigated.

Experimental setup, material structure, and instrumentation

System description

The experimental set up consisted, mainly, of two geometrically identical ordinary L-type SSs: one was a conventional

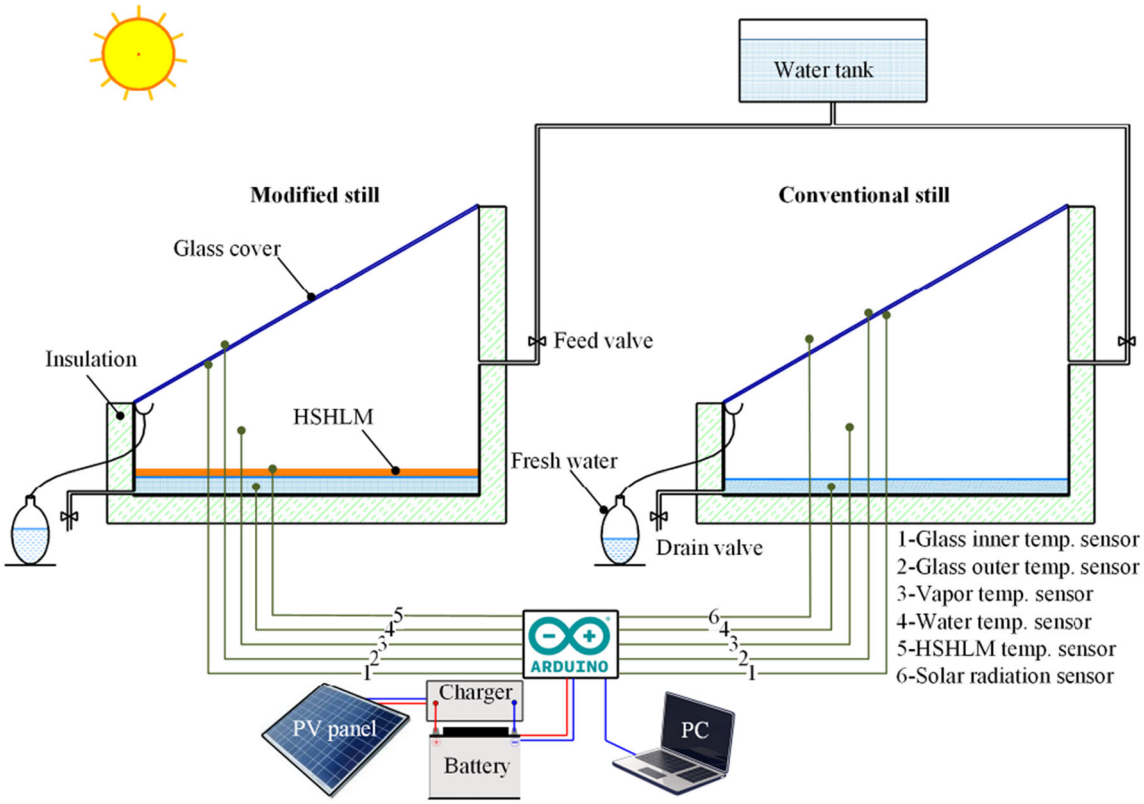

Fig. 1 Schematic diagram of the experimental set up

SS and the other was the modified one (provided with HSHLMs); as presented in schematic and photo in Figs. 1 and 2, respectively. Each SS was fabricated from 1.5-mm-thick galvanized steel and had a basin of (1 × 0.5) m with 0.44 m back side height and 0.15 m front wall height. In addition, for complete effective thermal performance, the whole internal surface of the basin was black-painted to maximize its solar absorptivity. To eliminate heat losses to the surrounding, the basin's sides and bottom walls were thermally insulated by 20 mm-thick foam having a thermal conductivity of (0.03 W/m K) (Li et al., 2019). In addition, the upper side facing the solar radiation was covered with 4-mm-thick

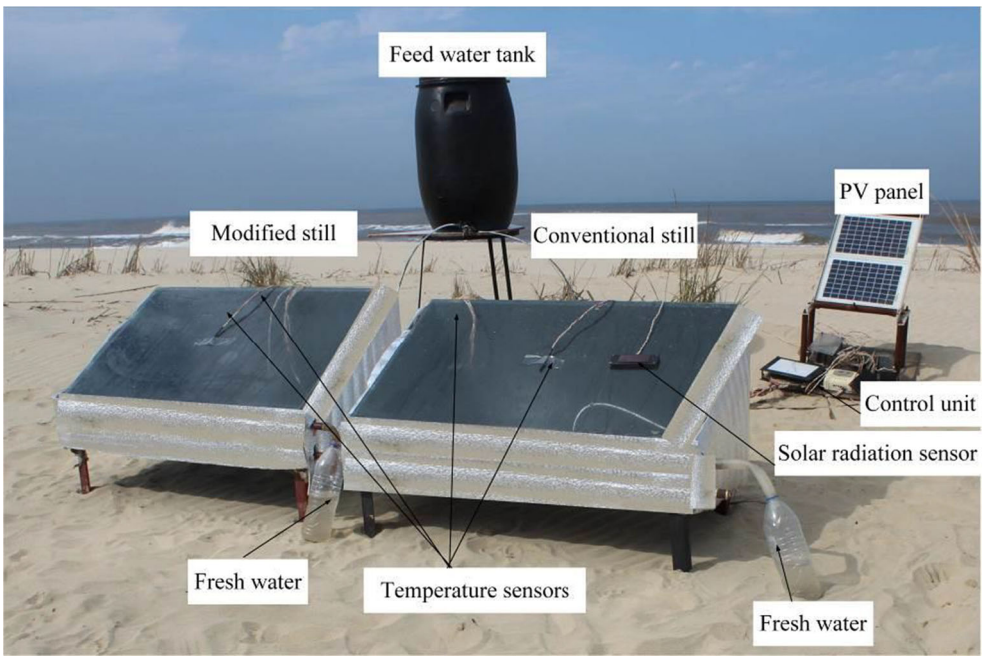

Fig. 2 Photo of the experimental set up

glass cover having emissivity and absorptivity of 0.88 and 0.05, respectively, and tilted at 30° to the horizontal plane facing South. The saline water was being collected from the Mediterranean Sea in a black-painted tank and being equally fed to the system through pipeline fitted with control valves.

The experiments were conducted on the beach of the Mediterranean Sea in Burullus city (latitude 31.58° N and longitude 30.98° E), Kafrelsheikh province, Egypt. The SSs were completely fabricated from locally available entities. The measurements were conducted from 8:30 am to 5:30 pm during sunny days.

Material structure

Three different materials were utilized to form the combinations used in each case of study: exfoliated graphite, wick, and carbon foam, with photos shown in Fig. 3 a, b, and c, respectively. All these materials had densities lower than that of bulk water, so, that guaranteed their suspension on the water surface as desired; except for the wick material that required using small hooks at the SS basin sides to suspend it on the water surface.

The absorptivity (%) spectra of the utilized materials: carbon foam, exfoliated graphite, wick, and bulk water; is shown in Fig. 3c that illustrates the spectra variation with different wavelengths. These variations were calculated through UV–V in the range from 400 to 1100 nm with a unity step. Through the whole range, carbon foam recorded the highest absorptivity at a stable average value of 99.04% with maximum and minimum values of 99.18 and 98.99%, respectively. Also, exfoliated graphite showed a stable absorptivity within the wavelengths range at an average value of 94.87% oscillating between 95.11 and 94.14%.

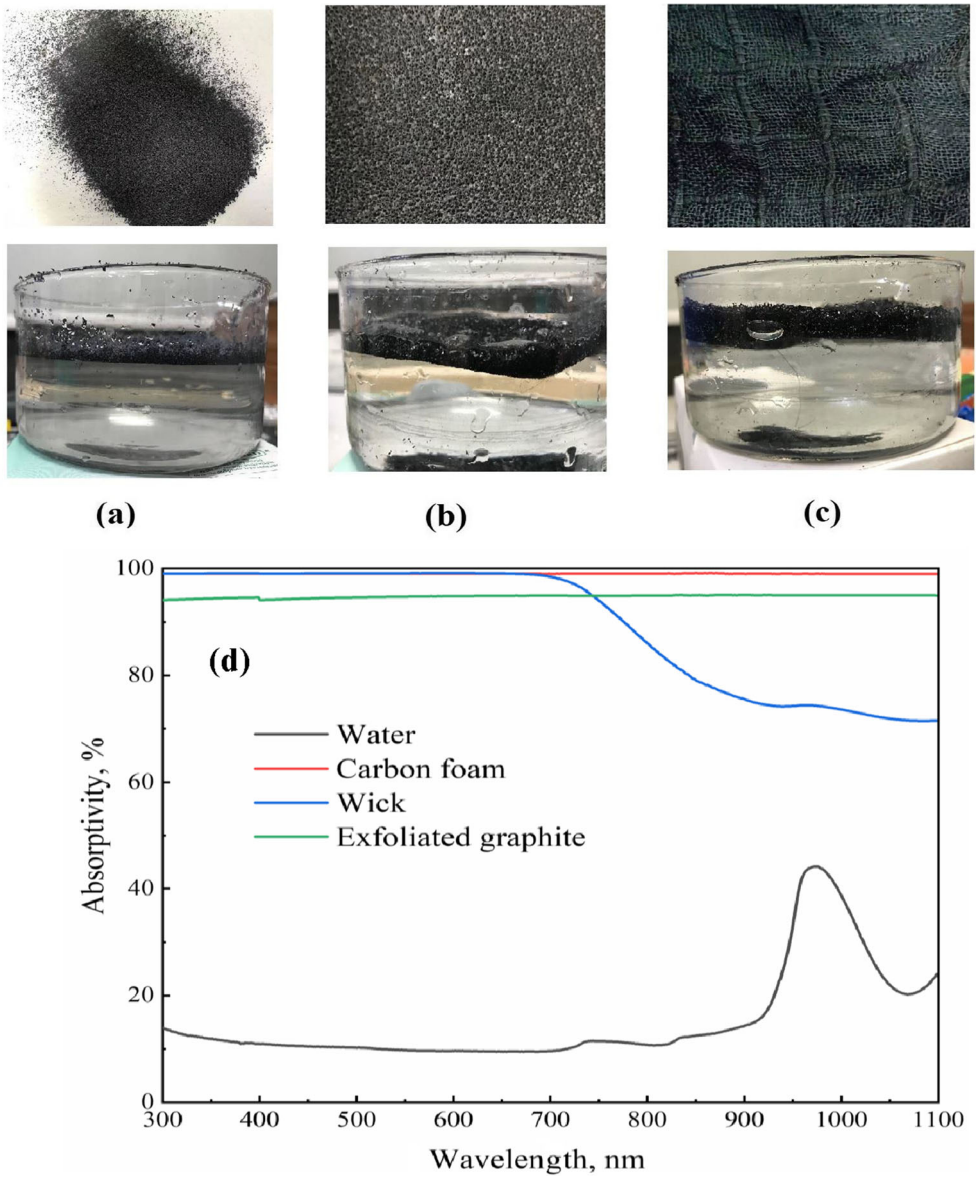

Fig. 3 Characteristics of utilized materials. **a** Photo of exfoliated graphite, **b** photo of carbon foam, **c** photo of wick, and **d** absorption spectra of the different materials and bulk water at different wavelengths

Whereas for a wick, it showed approximately the same absorptivity of carbon foam till wavelength of 710 nm, then, its absorptivity declined till a minimum value of 71.44% at 1081 nm, and then semi-stabilized till the final wavelength. Finally, bulk water had the lowest values of absorptivity of, approximately, on average, 10%, especially in low wavelengths, ranging from 400 to 750 nm. After that, bulk water absorptivity uplifted to the highest value of 44% at 975 nm and then decreased to 24% at the final wavelength.

For the proposed study, the effect of HSHLMs on the performance and productivity of SS, combinations of the previously mentioned materials, formed three types of HSHLMs that were utilized and involved in the system; as illustrated in Fig. 4. These types are formed as follows:

- Type A: Exfoliated graphite flakes over the wick.
- Type B: Carbon foam sandwiched between two wick layers.
- Type C: Exfoliated graphite flakes over carbon foam sandwiched between two wick layers.

Measuring devices and error analysis

The affecting parameters on the SSs' performance were evaluated through accurately calibrated electronic instrumentations. For temperature measurement, ten LM 35 temperature sensors with an accuracy of 0.1 °C were used with position shown in Fig. 1. These sensors were calibrated using AD590 calibration sensor to minimize the overall error percentage. For each SS, sensors were used to measure temperatures of water, vapor, and the inner and outer surface of glass cover. One sensor was used to measure temperature of HSHLM in the modified SS, and another was used to measure ambient air temperature. Moreover, a solar radiation sensor was positioned parallel to the glass cover to measure solar irradiance. This sensor was calibrated by positioning it at 30° (SS glass tilt angle) and changing its value according to the calibrated device (pyranometer). Both radiation and temperature sensors readouts were recorded to a memory card using Arduino Mega (with 15 analog inputs and 53 digital I/O pins) that was powered by a small PV-system consisting of PV panel, battery, and charger. Wind speed was measured using vane-type anemometer. The productivity was hourly collected in a sealed flask.

The values of range, accuracy, and error of different instrumentations are illustrated in Table 1 in which the minimum error is the ratio of least count to the minimum value of a measured quantity (Srithar 2003). For daily efficiency and productivity, the uncertainties were calculated according to (Holman 2001) and the resulting errors were ± 1.19 and ± 0.6%, for daily productivity and efficiency respectively.

Results and discussion

The effect of the usage of HSHLMs on SSs (modified SSs) performance was investigated and compared with a conventional

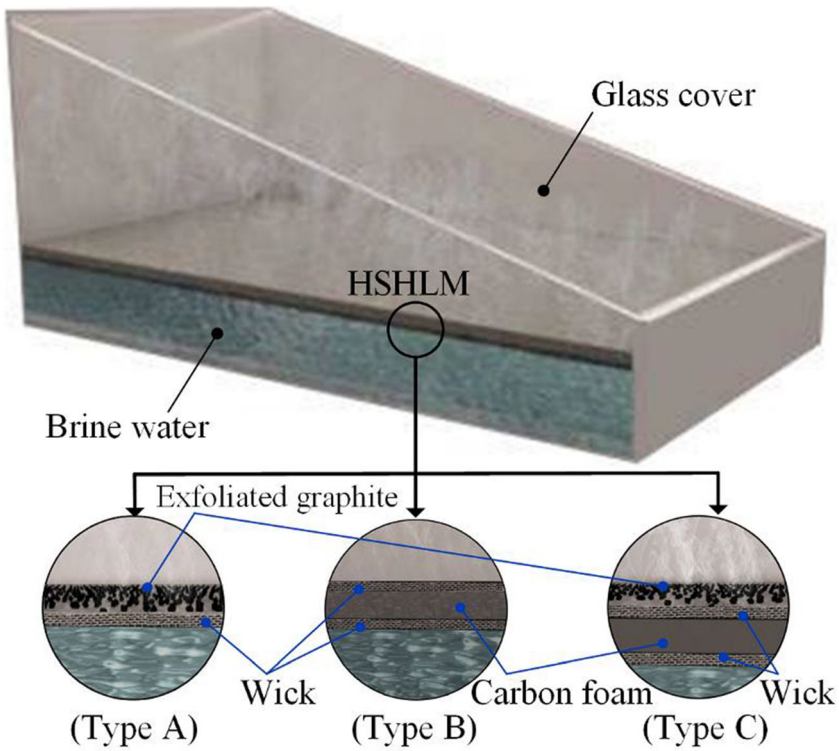

Fig. 4 Structure of the layers used in the modified solar still (HSHLM)

Table 1 Instrumentations uncertainty errors

Device	Range	Accuracy	Relative error (%)
Solar sensor with Arduino Mega	0–2000 W/m^2	± 1 W/m^2	0.156
LM 35 temperature sensor with Arduino Mega	0–300 °C	± 0.1 °C	0.2
Vane anemometer	± 0.1 m/s	0.4–30 m/s	2.5
Calibrated flask	0–2 l	± 0.005 l	1.176

SS performance operated at the same time. The actual data of solar radiation, air temperature, glass temperature, water temperature, and HSHLM temperature were displayed and recorded during the day using Arduino Mega. The water depth in each SS was kept constant with a value of 1 cm in each experiment.

Effect of exfoliated graphite flakes with wick

Figure 5 a depicts the variation of solar radiation, and temperatures of water, foam surfaces, and glass during the day of testing HSHLM of type A. The air temperature on this day had an average of 32 °C. The intensity of solar radiation reached its maximum value of 950 W/m^2 around 12:30 p.m. and declined gradually till sunset. Figure 5 a also illustrates the increase in exfoliated graphite surface temperature in the modified SS which reached a maximum value of 65.5 °C around 12:30 pm; while, the water temperature of the conventional SS reaches a maximum value of 60 °C at the same time. This difference in the maximum temperature is because of adding exfoliated graphite flakes and wick to the water surface. The

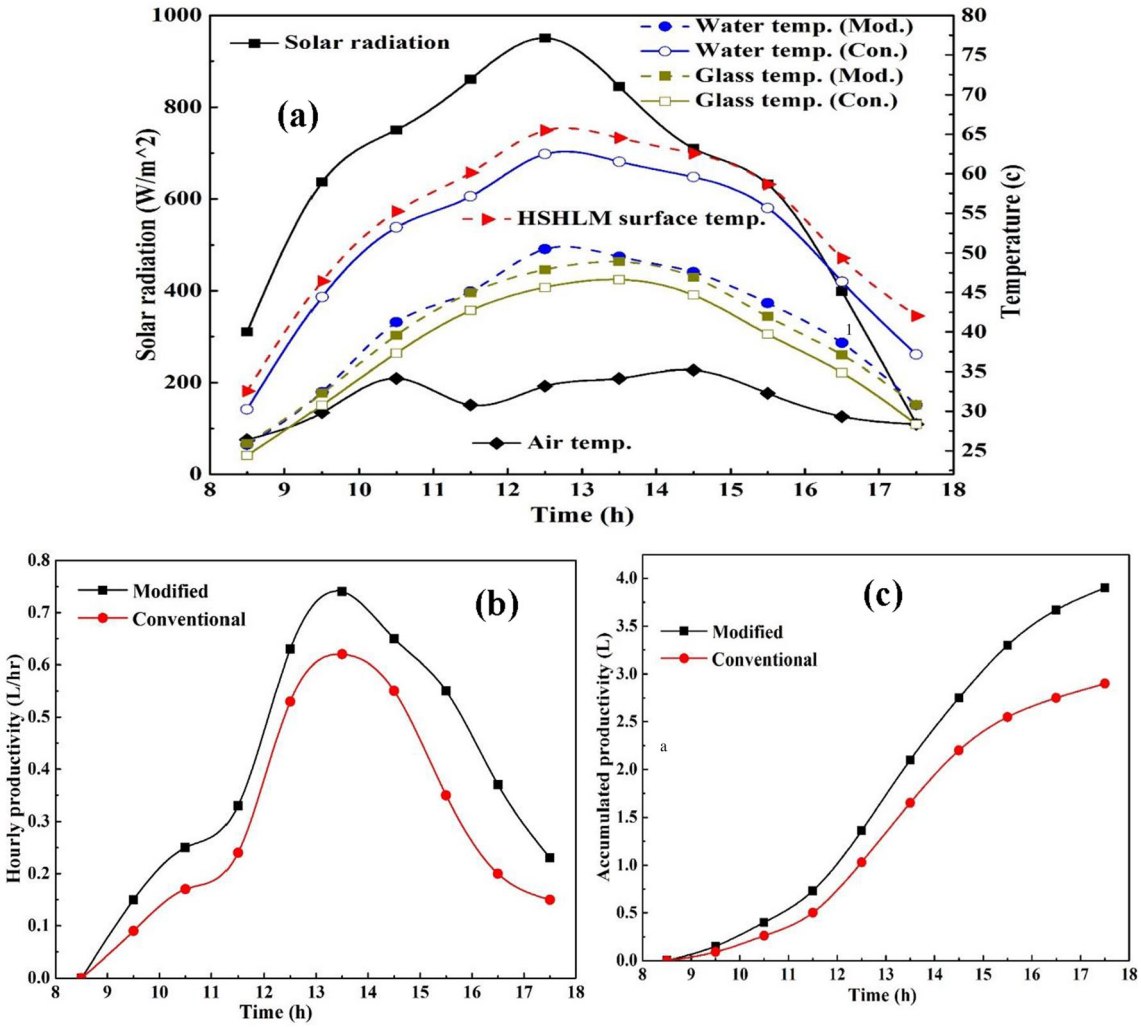

Fig. 5 Type A experiment. **a** Temperature and solar radiation variations. **b** Hourly productivity of SS with and without HSHLM. **c** Accumulated productivity of SS with and without HSHLM (15 Oct 2017)

difference between water temperature and glass temperature ranged from 1 to 3 °C and from 6 to 15 °C in the case of modified SS and conventional SS, respectively. As it is desirable to increase the temperature difference between the inner surface of the glass cover and the water surface as soon as possible to enhance the natural circulation inside the still as well as the condensation rate, the use of exfoliated graphite flakes has a beneficial effect to achieve this target.

Figure 5 a also shows that the water temperature of the conventional SS is greater than the water surface temperature of the modified one although the modified one had a greater productivity; this is because the HSHLM acts as insulation layer over water surface, and the water rises up by osmosis characteristic, and evaporation happens in this layer where the temperature is very high as there is no need to heating bulk water but only its surface. The results show that surface temperatures of the modified SS are higher than the conventional SS by about 5 °C. This is mainly due to the adding HSHLM on water surface which absorbed the heat and concentrated it on the water surface, which led to the rise in surface temperature and consequently evaporation of water was increased, which in turn increased the overall full-day productivity. The hourly productivity of both modified and conventional SSs is as shown in Fig. 5b. The hourly productivity was found to be 0.33 L and 0.24 L around 11:30 in the case of modified and conventional SS, respectively, i.e., there was an increase of 37.5% in hourly productivity of the modified SS over the conventional one. This percentage became larger around 15:30 and reached 57.14%. The accumulated productivity of both stills was recorded too as shown in Fig. 5c; it was 3.9 L/day and 2.9 L/day for the modified and conventional SS, respectively, with an increase of 34.5% in productivity during the day. Additionally, the efficiency was 36.9% and 26.8% for the modified and the conventional SS, respectively.

Effect of carbon foam with wick

Figure 6 a demonstrates the hourly variations of temperature and solar intensity when type B HSHLM was used. The average air temperature during the experiment was 25 °C. The solar intensity reached its maximum value of 945 W/m^2

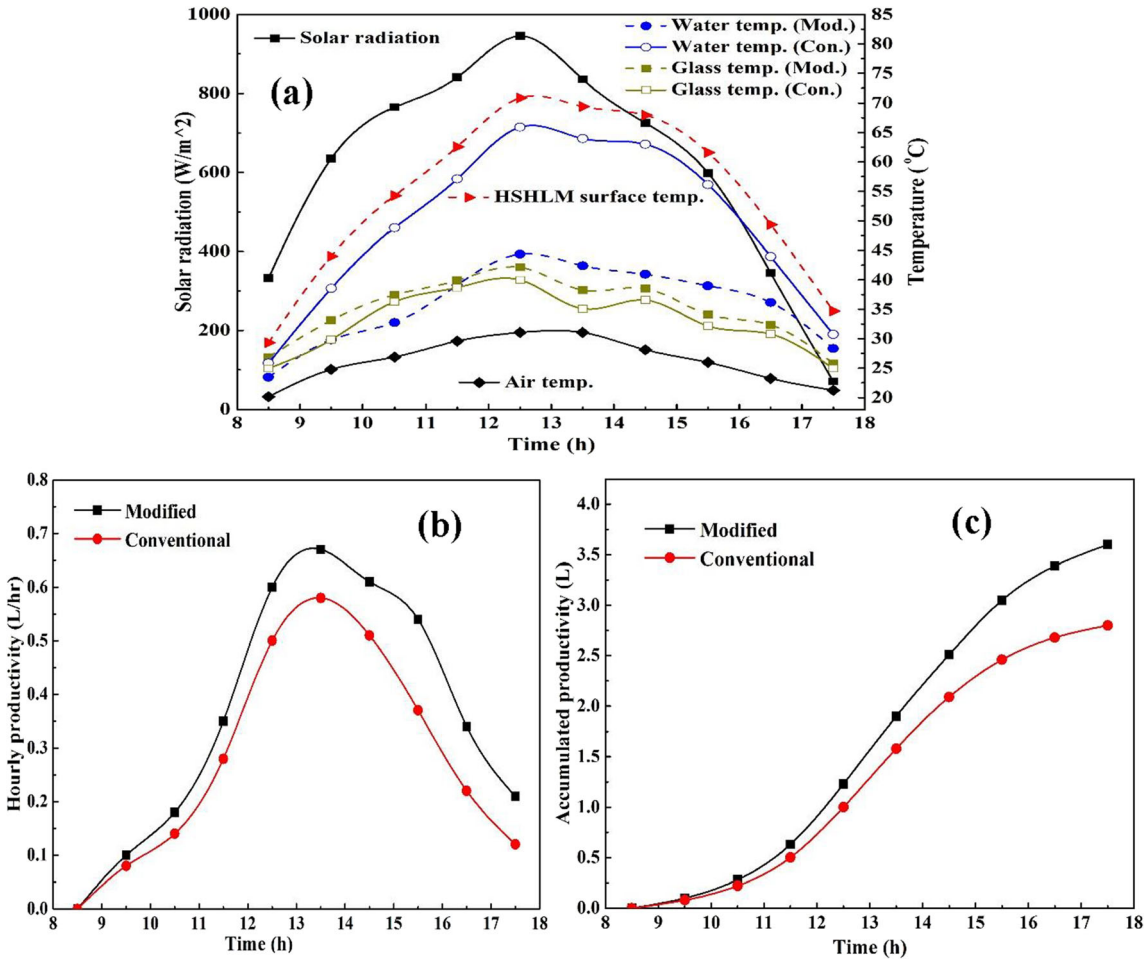

Fig. 6 Type B experiment. **a** Temperature and solar radiation variations. **b** Hourly productivity of SS with and without HSHLM. **c** Accumulated productivity of SS with and without HSHLM

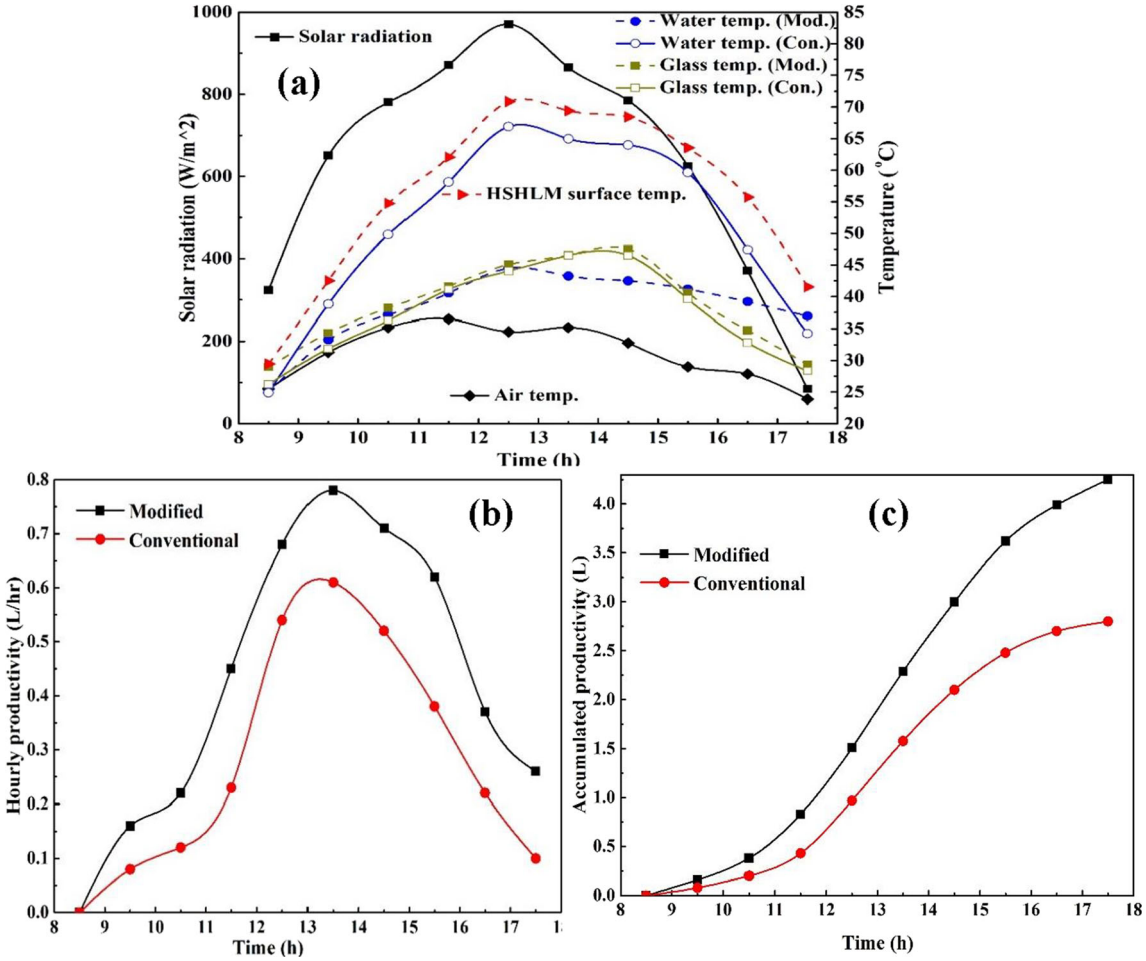

Fig. 7 Type C experiment. **a** Temperature and solar radiation variations. **b** Hourly productivity of SS with and without HSHLM. **c** Accumulated productivity of SS with and without HSHLM

around 12:30. Foam surface temperature, where evaporation takes place, rose until it reached a maximum value of 71 °C at 12:30 during the day due to the heat localization effect that carbon foam has on temperature rise whereas water temperature of the conventional SS reached a maximum value of 65 °C. The glass temperature of the modified SS was smaller than the conventional one at the beginning of the day, but it became greater around 11:30.

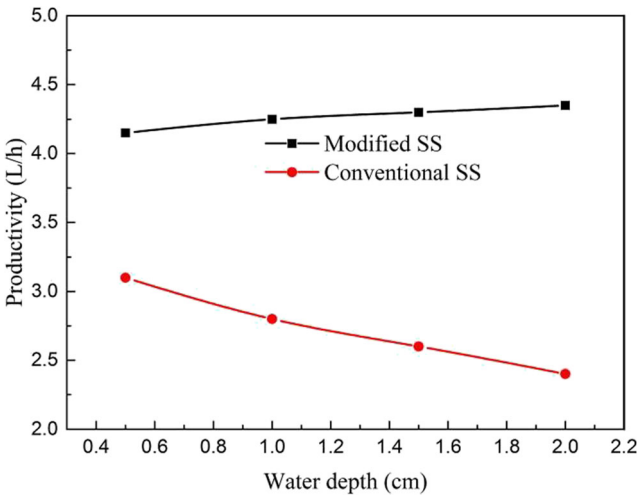

Fig. 8 The effect of the water depth on the SS accumulated productivity

Figure 6 b presents the hourly productivity of both modified and conventional SSs. The hourly productivity of modified SS is always greater than the conventional one during the day because of adding HSHLM to the water surface. Figure 6 c shows the accumulated productivity of both SSs as accumulated productivity of modified one was 3.6 L/day with an increase of 28.6% with respect to conventional SS which had productivity of 2.8 L/day. In addition, the efficiency of modified was 34.8 compared with 27% for conventional.

Effect of exfoliated graphite flakes and carbon foam with wick materials

Figure 7 a shows the variation of solar radiation, water temperature, foam surface temperature, and glass temperature during the day in the case of using type C HSHLM. During this experiment, the solar radiation reached a maximum intensity

Table 2 The SSs efficiency, accumulated productivity, and the increase in the productivity for the three HSHLM types

Date	Type A								Type B								Type C							
	06 Oct 2017		15 Oct 2017		18 Oct 2017		Average values		20 Oct 2017		21 Oct 2017		23 Oct 2017		Average values		25 Oct 2017		27 Oct 2017		01 Nov 2017		Average values	
Type	Con	Mod	Con	Mod	Con	Mod	Con	Mod	Con.	Mod	Con.	Mod.	Con.	Mod.	Con.	Mod.	Con.	Mod.	Con.	Mod.	Con.	Mod.	Con.	Mod.
Efficiency (%)	26.7	36.7	26.8	36.9	26.9	37	26.8	36.7	27.1	34.7	27	34.8	26.9	34.9	27	34.8	25.5	37.6	25.4	37.4	25.8	37.6	25.5	37.5
Accumulated prod. (L)	2.95	3.8	2.9	3.9	2.8	4	2.88	3.9	2.9	3.7	2.8	3.6	2.75	3.5	2.81	3.6	3	4.35	2.81	4.25	2.65	4.2	2.82	4.26

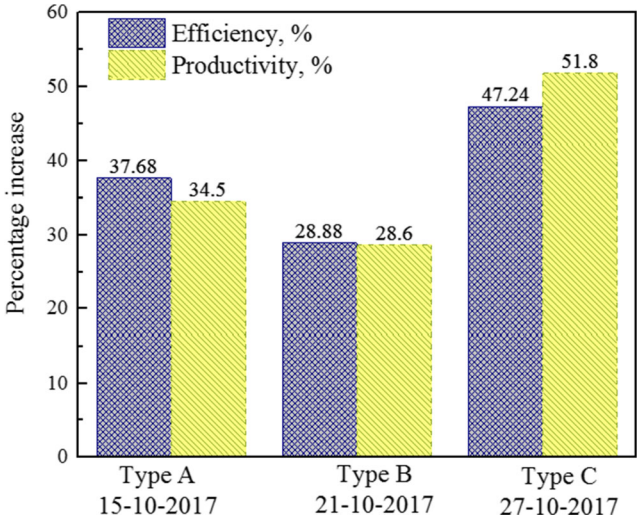

Fig. 9 The percentage increase in the productivity and efficiency for the modified SSs with three different HSHLM types compared with conventional SSs

of 970 W/m^2 around 12:30 and then it declined during the day until sunset. The average air temperature during the day of the experiment was about 31 °C as shown in Fig. 7a. The water surface temperature of the modified SS reached a maximum value of 53.5 °C around 12:30 pm then it declined during the rest of the day while it was 67 °C for the conventional one. The exfoliated graphite and foam surface, where evaporation takes place, reached a maximum value of 71 °C.

Figure 7 b shows the hourly productivity of the modified SS with and without HSHLM of type C. The productivity of the modified SS was always greater than the conventional SS during the day. There was a considerable increase in productivity after combining exfoliated graphite flakes and carbon foam as the accumulated productivity of the modified SS became 4.25 L/day with an increase of 51.8% with respect to the conventional that had the productivity of 2.8 L/day, as shown in Fig. 7c. Additionally, the efficiency was about 37.4% and 25.4% for the modified and conventional SS, respectively.

Effect of changing water depth for modified and conventional stills

Another experiment was done to study the effect of increasing water depth on the process of heat localization in the modified still with HSHLM type C, and the conventional one. The results showed that increasing the water depth of the modified SS has a positive effect on productivity in contrary to that in the conventional one (Kalidasa Murugavel et al. 2010) as shown in Fig. 8. When the water depth was 1 cm, the accumulated productivity was 2.8 L/day and 4.25 L/day for conventional and modified one type C, respectively. As the water depth increases, the productivity increases too as the heat localization process does not need to heat the bulk water in the

still, but it concentrates the heat on the surface of the water where the evaporation takes place.

Thermal performance

Daily efficiency η_d is used to assess the performance of the SS under investigation. It is defined as the sum of hourly productivity m_p multiplied by the latent heat L_w and divided by the absorber area A and the sum of hourly solar radiation $I(t)$(Dashtban and Tabrizi 2011; Kabeel et al. 2018):

$$\eta_d = \frac{\sum m_p \times L_w}{\sum A \times I(t)} \quad (1)$$

where the latent heat is calculated using the following equation (Dashtban and Tabrizi 2011; El-Dessouky and Ettouney 2002; Kabeel et al. 2018):

$$L_w = 10^3\left[2501.9{-}2.40706T_w + 1.192217 \times 10^{-3}T_w^2{-}1.5863 \times 10^{-5}T_w^3\right] \quad (2)$$

and T_w is the average temperature of basin water in conventional SS and HSHLM in modified SS.

The accumulated productivity of the freshwater, the percentage of productivity increase, and daily efficiency for the three types of HSHLM and conventional SS. The maximum SS efficiency was obtained using the type C HSHLM (37.6%) followed by type A (37%) and finally type B (34.8%); with an increase in the efficiency by about (47.24%) for type C, (37.68%) for type A, and (28.88%) for type B compared with the corresponding conventional SSs as shown in Fig. 9. As shown in Table 2, the average value of the accumulated productivity was found to be 3.9 L/day, 3.6 L/ day, and 4.25 L/ day for type A, type B, type C SSs, respectively. While the average accumulated productivity for the three corresponding conventional SS ranges between 2.8 and 2.9 L/day. The maximum average increase in the accumulated productivity was obtained using the type C HSHLM (51.3%) followed by type A (32.8%) and finally type C (27.1%). It has been inferred from the results that among the three investigated types of HSHLM, type C has shown the best productivity and thermal performance.

Compared with some other researchers' studies, the system showed good enhancement in both daily productivity and efficiency. In addition, the in-shore study is in good agreement with other inland ones as shown from Table 3. In other words, because of the rapprochement in the productivity of conventional SS in both studies in land area(other studies), and at beach side (current study), it can be considered that there is no significant effect of meteorological parameters at beach side on the performance of SS.. However, more intensive investigations should be conducted in future works to ensure this suggestion.

Cost analysis and water quality

The average cost ($) per 1 l of produced distilled water can be calculated regarding fixed installation (I), Table 4, annual variable running (R) costs, and expected lifetime (n); as total cost during operation lifetime $(C) = I + (n \times R)$$. In addition, the average total productivity during the operation lifetime (m_n)- $= i \times n \times m_d$, as i is operation days per year. According to (Kabeel 2009), it can be assumed that $n = 10$ years, $i =$ 340 day/year, and the values of $R = 0.3$ I. Hence, for example, the total cost of type C modified SS can be calculated as $C = (95) + (0.3 \times 10 \times 95) = 380$ $. Whereas, $m_n = 340 \times 10 \times 4.25 = 14{,}484$ L. Then, the cost per liter = 380/14,484 = 0.0262 $/L. In the same way, the cost per of conventional, modified type A, and modified type B are 0.033, 0.027, and 0.0294 $/L, respectively.

Table 3 Comparison between different cases of present work and various conventional SSs

Reference	Location	Type of SS	Average productivity (L/m^2 day)	Average efficiency (%)
Present study	Burullus city (latitude 31.58° N and longitude 30.98° E), Kafrelsheikh province, Egypt.	Conventional SS	2.83	26.5
		Modified type (A)	3.9	36.7
		Modified type (B)	3.6	34.8
		Modified type (C)	4.25	37.5
(Sharshir et al. 2019c)	Kafrelsheikh city (latitude 31.09° N and longitude 30. 95° E), Kafrelsheikh province, Egypt.	Conventional SS	3.2	30
(Omara et al. 2011)	Kafrelsheikh city (latitude 31.09° N and longitude 30. 95° E), Kafrelsheikh province, Egypt.	Conventional SS	3.07	34
(Omara et al. 2014)	Kafrelsheikh city (latitude 31.09° N and longitude 30. 95° E), Kafrelsheikh province, Egypt.	Conventional SS	3.1	Not given

Table 4 Fixed installation costs of different investigated SSs

Unit	Conventional still	Type A	Type B	Type C
Fixed installation I ($)	80	90	90	95
Annual variable running R ($/year)	24	27	27	28.5
Average productivity during the lifetime m_n (L)	9656	13,260	12,240	14,484

Additionally, saline and fresh water qualities were measured to ensure its values agree with the acceptable range. It was found that the evaluated samples witnessed a drop in both total dissolved solids (TDS) and the power of hydrogen (pH) values. TDS values witnessed a sharp drop from 35,350 to 80 mg/L; before and after the desalination process, respectively. Whereas, the pH values were 7.8 and 7.0 for saline and fresh water, respectively. According to World Health Organization (WHO) (Organization 2004), these values of water quality is acceptable.

Conclusions

In the current experimental work, a new technique for improving the performance of solar stills (SSs) via utilizing three different types of a hybrid structure of heat localization materials (HSHLM) was proposed. The three types were exfoliated graphite flakes with wick (type A), carbon foam with wick (type B), and exfoliated graphite flakes with wick and carbon foam (type C). The effect of the three HSHLM types on the SS performance was investigated as well as changing the water depth on it. As the result, the following major outcomes can be concluded:

- The HSHLMs helped in localizing the heat at the water surface; and hence, that led to an increase in the evaporation rate and minimizes the heat losses. So, The hourly productivity and accumulated productivity of the modified SS were always greater than the conventional one.
- The maximum productivity achieved in case HSHLM type C was 4.25 L/day (an increase of 51.8% compared with conventional SS).
- The efficiency of the modified SS was found to be 37.4%, 36.9%, and 34.8%, when using type C, type A, and type B, respectively.
- The productivity of the modified SS with HSHLM significantly increased when the water depth increases contrary to conventional SSs.

Nomenclatures A, absorber area, (m^2); C, total cost of solar still operation during its lifetime, ($); I, fixed installation cost, ($); I(t), hourly solar radiation intensity (W/m^2); i, number of annual operation days (day/yr); L_w, latent heat of water (kJ/kg); m_d, average daily productivity (kg/ m^2 day); m_n, average total productivity during the operation lifetime (kg); m_p, hourly freshwater (L/m^2 h); n, number of lifetime years (yr); R, running variable cost ($/yr); T_w, verage temperature of basin water (°C)

Abbreviations η_d, daily efficiency; d, daily; HSLM, hybrid structure of heat localization material; PCM, phase change material; PV, photovoltaic; pH, power of hydrogen; a measure of hydrogen ion concentration evaluating the acidity or alkalinity of a solution; P, productivity; SS, solar still; TDS, total dissolved solids; w, water

References

Abujazar MSS, Fatihah S, Ibrahim IA, Kabeel AE, Sharil S (2018) Productivity modelling of a developed inclined stepped solar still system based on actual performance and using a cascaded forward neural network model. J Clean Prod 170:147–159

Arunkumar T, Kabeel AE, Raj K, Denkenberger D, Sathyamurthy R, Ragupathy P, Velraj R (2018) Productivity enhancement of solar still by using porous absorber with bubble-wrap insulation. J Clean Prod 195:1149–1161

Ayoub GM, Malaeb L (2014) Economic feasibility of a solar still desalination system with enhanced productivity. Desalination 335:27–32

Balachandran, G.B., David, P.W., Mariappan, R.K., Kabeel, A.E., Athikesavan, M.M., Sathyamurthy, R., 2019. Improvising the efficiency of single-sloped solar still using thermally conductive nanoferric oxide. Environ Sci Pollut Res, 1-14

Balachandran, G.B., David, P.W., Vijayakumar, A.B.P., Kabeel, A.E., Athikesavan, M.M., Sathyamurthy, R., Enhancement of PV/T-integrated single slope solar desalination still productivity using water film cooling and hybrid composite insulation. Environmental Science and Pollution Research, 1–12

Dashtban M, Tabrizi FF (2011) Thermal analysis of a weir-type cascade solar still integrated with PCM storage. Desalination 279:415–422

Dsilva Winfred Rufuss D, Suganthi L, Iniyan S, Davies PA (2018) Effects of nanoparticle-enhanced phase change material (NPCM) on solar still productivity. J Clean Prod 192:9–29

El-Dessouky HT, Ettouney HM (2002) Fundamentals of salt water desalination. Elsevier

El-Samadony YAF, Kabeel AE (2014) Theoretical estimation of the optimum glass cover water film cooling parameters combinations of a stepped solar still. Energy 68:744–750

Elshamy SM, El-Said EMS (2018) Comparative study based on thermal, exergetic and economic analyses of a tubular solar still with semi-circular corrugated absorber. J Clean Prod 195:328–339

Elsheikh AH, Sharshir SW, Ahmed Ali MK, Shaibo J, Edreis EMA, Abdelhamid T, Du C, Haiou Z (2019) Thin film technology for solar steam generation: a new dawn. Sol Energy 177:561–575

Elsheikh AH, Sharshir SW, Mostafa ME, Essa FA, Ahmed Ali MK (2018) Applications of nanofluids in solar energy: a review of recent advances. Renew Sust Energ Rev 82:3483–3502

Ghasemi H, Ni G, Marconnet AM, Loomis J, Yerci S, Miljkovic N, Chen G (2014) Solar steam generation by heat localization. Nat Commun 5:4449

Hassan H, Abo-Elfadl S (2017) Effect of the condenser type and the medium of the saline water on the performance of the solar still in hot climate conditions. Desalination 417:60–68

Holman, J.P., 2001. Experimental methods for engineers

Kabeel AE (2009) Performance of solar still with a concave wick evaporation surface. Energy 34:1504–1509

Kabeel AE, Abdelgaied M, Eisa A (2018) Enhancing the performance of single basin solar still using high thermal conductivity sensible storage materials. J Clean Prod 183:20–25

Kabeel AE, Arunkumar T, Denkenberger DC, Sathyamurthy R (2017a) Performance enhancement of solar still through efficient heat exchange mechanism – a review. Appl Therm Eng 114:815–836

Kabeel, A.E., El-Agouz, E.-S., Athikesavan, M.M., Ramalingam, R.D., Sathyamurthy, R., Prakash, N., Prasad, C., (2019a) Comparative analysis on freshwater yield from conventional basin-type single slope solar still with cement-coated red bricks: an experimental approach. Environmental science and pollution research, 1-11

Kabeel AE, Sathyamurthy R, Sharshir SW, Muthumanokar A, Panchal H, Prakash N, Prasad C, Nandakumar S, El Kady MS (2019b) Effect of water depth on a novel absorber plate of pyramid solar still coated with TiO2 nano black paint. J Clean Prod 213:185–191

Kabeel AE, Sharshir SW, Abdelaziz GB, Halim MA, Swidan A (2019c) Improving performance of tubular solar still by controlling the water depth and cover cooling. J Clean Prod 233:848–856

Kabeel AE, Teamah MA, Abdelgaied M, Abdel Aziz GB (2017b) Modified pyramid solar still with v-corrugated absorber plate and PCM as a thermal storage medium. J Clean Prod 161:881–887

Kalidasa Murugavel K, Sivakumar S, Riaz Ahamed J, Chockalingam KKSK, Srithar K (2010) Single basin double slope solar still with minimum basin depth and energy storing materials. Appl Energy 87: 514–523

Khare VR, Singh AP, Kumar H, Khatri R (2017) Modelling and performance enhancement of single slope solar still using CFD. Energy Procedia 109:447–455

Li C, Goswami Y, Stefanakos E (2013) Solar assisted sea water desalination: a review. Renew Sust Energ Rev 19:136–163

Li C, Jiang D, Huo B, Ding M, Huang C, Jia D, Li H, Liu C, Liu J (2019) Scalable and robust bilayer polymer foams for highly efficient and stable solar desalination. Nano Energy 60

Liu C, Huang J, Hsiung CE, Tian Y, Wang J, Han Y, Fratalocchi A (2017) High-performance large-scale solar steam generation with nanolayers of reusable biomimetic nanoparticles. Adv Sustain Syst:1

Madani AA, Zaki GM (1995) Yield of solar stills with porous basins. Appl Energy 52:273–281

Mousa H, Gujarathi AM (2016) Modeling and analysis the productivity of solar desalination units with phase change materials. Renew Energy 95:225–232

Nisan S, Benzarti N (2008) A comprehensive economic evaluation of integrated desalination systems using fossil fuelled and nuclear energies and including their environmental costs. Desalination 229: 125–146

Omara ZM, Hamed MH, Kabeel AE (2011) Performance of finned and corrugated absorbers solar stills under Egyptian conditions. Desalination 277:281–287

Omara ZM, Kabeel AE, Younes MM (2014) Enhancing the stepped solar still performance using internal and external reflectors. Energy Convers Manag 78:876–881

Organization, W.H (2004) Guidelines for drinking-water quality. World Health Organization

Peng G, Deng S, Sharshir SW, Ma D, Kabeel AE, Yang N (2020) High efficient solar evaporation by airing multifunctional textile. Int J Heat Mass Transf 147:118866

Peng G, Ding H, Sharshir SW, Li X, Liu H, Ma D, Wu L, Zang J, Liu H, Yu W, Xie H, Yang N (2018) Low-cost high-efficiency solar steam generator by combining thin film evaporation and heat localization: both experimental and theoretical study. Appl Therm Eng 143: 1079–1084

Rashidi S, Akar S, Bovand M, Ellahi R (2018) Volume of fluid model to simulate the nanofluid flow and entropy generation in a single slope solar still. Renew Energy 115:400–410

Rodriguez-Narvaez OM, Peralta-Hernandez JM, Goonetilleke A, Bandala ER (2017) Treatment technologies for emerging contaminants in water: a review. Chem Eng J 323:361–380

Salgot M, Folch M (2018) Wastewater treatment and water reuse. Curr Opin Environ Sci Health 2:64–74

Samuel Hansen R, Kalidasa Murugavel K (2017) Enhancement of integrated solar still using different new absorber configurations: an experimental approach. Desalination 422:59–67

Shalaby SM, El-Bialy E, El-Sebaii AA (2016) An experimental investigation of a v-corrugated absorber single-basin solar still using PCM. Desalination 398:247–255

Sharshir SW, El-Samadony MOA, Peng G, Yang N, Essa FA, Hamed MH, Kabeel AE (2016a) Performance enhancement of wick solar still using rejected water from humidification-dehumidification unit and film cooling. Appl Therm Eng 108:1268–1278

Sharshir SW, Elkadeem MR, Meng A (2020) Performance enhancement of pyramid solar distiller using nanofluid integrated with v-corrugated absorber and wick: an experimental study. Appl Therm Eng 168:114848

Sharshir SW, Ellakany YM, Eltawil MA (2019a) Exergoeconomic and environmental analysis of seawater desalination system augmented with nanoparticles and cotton hung pad. J Clean Prod:119180

Sharshir SW, Elsheikh AH, Peng G, Yang N, El-Samadony MOA, Kabeel AE (2017a) Thermal performance and exergy analysis of solar stills – a review. Renew Sust Energ Rev 73:521–544

Sharshir SW, Elsheikhd AH, Edreise EM, Alig MKA, Sathyamurthyh R, Kabeel AE, Zanga J, Yangb NJD, Treatment W (2019b) Improving the solar still performance by using thermal energy storage materials: a review of recent developments. 165, 1-15

Sharshir SW, Kandeal AW, Ismail M, Abdelaziz GB, Kabeel AE, Yang N (2019c) Augmentation of a pyramid solar still performance using evacuated tubes and nanofluid: experimental approach. Appl Therm Eng 160:113997

Sharshir SW, Peng G, Elsheikh AH, Eltawil MA, Elkadeem MR, Dai H, Zang J, Yang N (2019d) Influence of basin metals and novel wick-metal chips pad on the thermal performance of solar desalination process. J Clean Prod 119224

Sharshir SW, Peng G, Wu L, Essa FA, Kabeel AE, Yang N (2017b) The effects of flake graphite nanoparticles, phase change material, and film cooling on the solar still performance. Appl Energy 191:358–366

Sharshir SW, Peng G, Wu L, Yang N, Essa FA, Elsheikh AH, Mohamed SIT, Kabeel AE (2017c) Enhancing the solar still performance using nanofluids and glass cover cooling: experimental study. Appl Therm Eng 113:684–693

Sharshir SW, Peng G, Yang N, El-Samadony MOA, Kabeel AE (2016b) A continuous desalination system using humidification – dehumidification and a solar still with an evacuated solar water heater. Appl Therm Eng 104:734–742

Sharshir SW, Peng G, Yang N, Eltawil MA, Ali MKA, Kabeel AE (2016c) A hybrid desalination system using humidification-dehumidification and solar stills integrated with evacuated solar water heater. Energy Convers Manag 124:287–296

Sharshir SW, Yang N, Peng G, Kabeel AE (2016d) Factors affecting solar stills productivity and improvement techniques: a detailed review. Appl Therm Eng 100:267–284

Srithar K (2003) Studies on solar augmented evaporation systems for tannery effluent (Soak liquor). PhD thesis, Indian Institute of Technology, Madras

Su W, Darkwa J, Kokogiannakis G (2015) Review of solid–liquid phase change materials and their encapsulation technologies. Renew Sust Energ Rev 48:373–391

T.C P, Sharma SK, Kennedy M (2018) Nanoparticles in household level water treatment: an overview. Sep Purif Technol 199:260–270

Wang X, He Y, Cheng G, Shi L, Liu X, Zhu J (2016) Direct vapor generation through localized solar heating via carbon-nanotube nanofluid. Energy Convers Manag 130:176–183

Xu N, Hu X, Xu W, Li X, Zhou L, Zhu S, Zhu J (2017) Mushrooms as efficient solar steam-generation devices. Adv Mater 29:1606762

Xue G, Liu K, Chen Q, Yang P, Li J, Ding T, Duan J, Qi B, Zhou J (2017) Robust and low-cost flame-treated wood for high-performance solar steam generation. ACS Appl Mater Interfaces 9:15052–15057

Zhang Y, Sivakumar M, Yang S, Enever K, Ramezanianpour M (2018) Application of solar energy in water treatment processes: a review. Desalination 428:116–145